ELSEVIER

Computational Materials Science 16 (1999) 355–361

COMPUTATIONAL MATERIALS SCIENCE

Simulation of crystal plasticity under dynamic loading

R.R. Balokhonov *, P.V. Makarov, V.A. Romanova, I.Yu. Smolin

Institute of Strength Physics and Materials Science, Siberian Branch, Russian Academy of Sciences, 2/1 pr. Academicheskii, 634021 Tomsk, Russian Federation

Abstract

Phenomenological constitutive equations of relaxation type have been constructed and applied to simulate plastic deformation of heterogeneous media. Both the dislocation kinetics and the viscous model with function of relaxation times were used to calculate the plastic strain rate. The deformation at the meso scale level of polycrystals subjected to dynamic loading (including shock waves) has been numerically investigated. The results obtained are reported and discussed.

Keywords: Constitutive equations; Stress relaxation; Viscous stress; Plasticity; Polycrystals; Mesovolume; Strain localisation; Numerical modelling

1. Introduction

Stress relaxation in dynamically loaded material is most intensive and should be taken into consideration in numerical modelling. Nonequilibrium (viscous) stress seems to be important, especially through the shock wave front [1] and should be correctly described by the constitutive equations. For instance, the nonequilibrium stress for aluminium alloys and steels loaded by weak shock waves (5–10 GPa) is comparable with the Hugoniout yield stress. For Al60061-T6 shocked by 9 GPa, the Hugoniout yield point is 0.12 GPa and the nonequilibrium stress is 0.1 GPa through the steady wave front [2].

Thus, constitutive equations used for modelling the dynamic loading should include the nonequilibrium shear stress and, hence, should be formulated in a relaxation form.

Let us define total stress as

$$\sigma_{ij} = -P\delta_{ij} + s^{e}_{ij} + s^{v}_{ij}, \tag{1}$$

where P is the pressure, s^{e}_{ij} the elastic (equilibrum) stress deviator and s^{v}_{ij} is the nonequilibrium (viscous) stress deviator.

Let us write the constitutive equations for plane shock waves and uniaxial tension in terms of the main shear stress $\tau = \frac{1}{2}(\sigma_1 - \sigma_2)$ and the main plastic strain rate $\dot{\gamma}^{p} = \frac{1}{2}(\dot{\varepsilon}^{p}_1 - \dot{\varepsilon}^{p}_2)$. In the main axis these are:

$$\dot{\tau} = \mu\left(\dot{\varepsilon}^{T}_1 - 2\dot{\gamma}^{p}\right), \qquad \sigma_1 = -P + s_1 = -P + \tfrac{4}{3}\tau,$$

$$\dot{\varepsilon}^{T}_2 = \dot{\varepsilon}^{T}_3 = 0 \tag{2}$$

for plane shock wave and

* Corresponding author. Tel.: +7-3822-286-876; fax: +7-3822-259-576.

E-mail address: rusy@ispms.tsc.ru (R.R. Balokhonov).

0927-0256/99/$ - see front matter
PII: S0927-0256(99)00078-6

$$\dot{\sigma}_1 = E\dot{\varepsilon}_1^{\mathrm{e}} = E\left(\dot{\varepsilon}_1^{\mathrm{T}} - \tfrac{4}{3}\dot{\gamma}^{\mathrm{p}}\right), \quad \dot{\varepsilon}_2^{\mathrm{T}} = \dot{\varepsilon}_3^{\mathrm{T}},$$
$$\sigma_2 = \sigma_3 = 0, \qquad \tau = \tfrac{1}{2}\sigma_1 \tag{3}$$

for uniaxial tension, with both the hypothesis of plastic incompressibility $\dot{\varepsilon}_1^{\mathrm{p}} + \dot{\varepsilon}_2^{\mathrm{p}} + \dot{\varepsilon}_3^{\mathrm{p}} = 0$ and $\dot{\varepsilon}_i^{\mathrm{T}} = \dot{\varepsilon}_i^{\mathrm{e}} + \dot{\varepsilon}_i^{\mathrm{p}}$ $(i = 1, 2, 3)$ being taken into account. Here $\dot{\varepsilon}_i^{\mathrm{T}}$ is the total strain rate, $\dot{\varepsilon}_i^{\mathrm{e}}$ and $\dot{\varepsilon}_i^{\mathrm{p}}$ are the elastic and plastic strain rates, respectively.

Thus, the nonequilibrium stress s_{ij}^{v} is determined by the law of relaxation, particularly by the rate of accumulation of plastic shear $\dot{\gamma}^{\mathrm{p}}$ in Eqs. (2) and (3). In other words, the increment of stress for the two special cases in relaxation equations (2) and (3) specifies both elastic and nonequilibrium parts of the total stress increment under dynamic loading. This approach will be extended to include common cases of 2D and 3D deformation. The constitutive equations (2) and (3) will be used for simulation of model experiments to define the model parameters that specify plastic strain rate $\dot{\gamma}^{\mathrm{p}}$.

This approach seems to be especially important for the description of deformation of rate-sensitive materials. If the time of relaxation is essentially lesser than the average characteristic time of loading of macro or meso volumes of a material, the model of instant relaxation (reduction of shear stress on an equilibrium yielding surface) is frequently used. It is also used for materials which show a weak sensitivity to strain rate. The model is a specific case of the approach suggested.

Shock wave loading differs essentially from other types of loading by the characteristic time of loading. The deformation rate through the shock wave front is very high and commensurable with relaxation rate, and the nonequilibrium stress is considerable. Inner structures of shocked and quasi-statically loaded materials evolve in different ways. For instance, a cellular structure was found in aluminium and its alloys shocked by 5–15 GPa and while it was not observed under tension even up to several tens of percent. Twins are observed for a number of shocked materials that do not twinned under lower rates of deformation [2]. To take into account these peculiarities, both the dislocation kinetics parameters and the function of relaxation time were determined from the experiments at different rates of loading, such as plane shock wave propagation and tension.

The relaxation constitutive equations (2) and (3) can be numerically solved, provided the plastic shear rate $\dot{\gamma}^{\mathrm{p}}$ is defined. Both the dislocation kinetics and viscous phenomenological model with relaxation time will be used for that.

2. Dislocation model of medium

Let us define the plastic strain rate $\dot{\gamma}^{\mathrm{p}}$ in constitutive equations (2) and (3) as a flow of similar defects in the Orowan law. This is considered in [3]:

$$\dot{\gamma}^{\mathrm{p}} = |\mathbf{g}| b N f \mathsf{v}. \tag{4}$$

Since the movement of defects occurs mainly in the planes of maximum shear stress [2], the orientation factor $|\mathbf{g}|$ in (4) is equal to 0.5. The expressions for the dislocation density N were obtained in the form [4]

$$N = N^* + (N_0 - N^*)\exp\left(-\frac{A}{|\mathbf{g}|b}\gamma_k^{\mathrm{p}}\right), \tag{5}$$

where N^* can be interpreted as a limiting dislocation density under loading and $\gamma_k^{\mathrm{p}} = \int_0^t |\dot{\gamma}^{\mathrm{p}}|\,\mathrm{d}t$ describes the strain history. A similar expression is written for the fraction of mobile dislocations:

$$f = f^* + (f_0 - f^*)\cdot\exp\left(-\frac{B}{|\mathbf{g}|b}(\gamma_k^{\mathrm{p}} - \gamma_{kr}^{\mathrm{p}})\right). \tag{6}$$

Given $\gamma_{kr}^{\mathrm{p}} = \gamma_k^{\mathrm{p}}(1 - N/N^*)$ at the change of $(\tau - \tau_{bs})$ sign, the calculations would describe the nonideal Bauschinger effect correctly.

Calculations under different strain rates show that there is a good reason to use the following semi-empirical expression for dislocation velocities:

$$\mathsf{v} = \mathsf{v}_0 \cdot \frac{ST^2}{1 + ST^2}, \quad ST = (\tau - \tau_0')/\beta_1, \tag{7}$$

where τ_0' is the value up to which the stress relaxes.

3. Strain hardening

Both the remote back stress and meso substructure formation depress the defect movement and result in the work hardening.

$$\tau_0'(\gamma^{\mathrm{p}}) = \tau_0 + \tau_{bs} + \sum_j K_j P_j(\gamma^{\mathrm{p}}), \tag{8}$$

where

$$\tau_{bs} = \alpha\mu b\sqrt{N} \tag{9}$$

and

$$P_j(\gamma^{\mathrm{p}}) = \int_0^{\gamma^{\mathrm{p}}} \lambda_j \cdot \exp\{\psi - \exp\psi\}\,\mathrm{d}\gamma^{\mathrm{p}}, \quad \psi = -\lambda_j \cdot (\gamma^{\mathrm{p}} - \gamma_j^{\mathrm{p}}) \tag{10}$$

is of a meaning of the probability of meso substructure formation at the corresponding deformation stage, γ_j^{p} is the degree of deformation corresponding to the beginning of certain meso substructure formation ($j = 1, 2, 3\ldots$ – for cells, bands, fragmented structures, respectively). Thus, relations (4)–(7) determine the plastic strain rate in (2) and (3) through the evolution of dislocation continuum, and Eq. (8) determines the dislocation (9) and meso substructure (10) strain hardening.

4. Model of medium with function of relaxation time

According to the second approach, the plastic strain rate $\dot{\gamma}^{\mathrm{p}}$ in Eqs. (2) and (3) may be associated with the viscous stress through the function of relaxation time (or viscosity factor η). Using Eq. (1), let us write for shear stress:

$$\tau = \tau^{\mathrm{e}} + \tau^{\mathrm{v}}. \tag{11}$$

The first term in (11) has a meaning of the yield point under strain hardening (8) and the second term in (11) may be determined as

$$\tau^{\mathrm{v}} = 2\eta\dot{\gamma}^{\mathrm{p}}. \tag{12}$$

Then, for 1D simulation we have

$$\dot{\gamma}^{\mathrm{p}} = \frac{\tau - \tau_0'}{2\eta}. \tag{13}$$

The viscosity factor is the function of the plastic strain γ^{p} and the shear stress τ. Using the experimental data and profiles calculated by means of the above dislocation kinetics, the function was constructed for AL6061-T6 alloy

$$\eta = \left[\exp\left(\frac{0.352}{\sigma_{\mathrm{eff}} - 0.24} + \frac{0.01751}{\varepsilon_{\mathrm{eff}}^{\mathrm{p}} + 0.005} - 11.0\right)\right] \cdot 10^{-4}\ \text{GPa s}, \tag{14}$$

where $\sigma_{\mathrm{eff}} = 2\tau$ and $\varepsilon_{\mathrm{eff}}^{\mathrm{p}} = \frac{4}{3}\gamma^{\mathrm{p}}$.

5. Constitutive equations of relaxation type for 2D and 3D simulation

Let us write the total deviatoric stress in the relaxation form

$$\dot{S}_{ij} = 2\mu\left(\dot{\varepsilon}_{ij}^{\mathrm{T}} - \frac{1}{3}\frac{\dot{V}}{V}\delta_{ij} - \dot{\varepsilon}_{ij}^{\mathrm{p}}\right), \tag{15}$$

where μ is the shear modulus; V the specific volume; $\dot{\varepsilon}_{ij}^{\mathrm{T}}$ the total strain rates and $\dot{\varepsilon}_{ij}^{\mathrm{p}}$ are the plastic strain rates. Here $\dot{\varepsilon}_{ij}^{\mathrm{p}}$ are defined according to the flow theory using the von Mises yield criterion [5]:

$$\dot{\varepsilon}_{ij}^{\mathrm{p}} = \frac{3}{2}\frac{\dot{\varepsilon}_{\mathrm{eff}}^{\mathrm{p}}}{\sigma_{\mathrm{eff}}} S_{ij}, \tag{16}$$

where

$$\dot{\varepsilon}_{\mathrm{eff}}^{\mathrm{p}} = \frac{\sqrt{2}}{3}\left(\left(\dot{\varepsilon}_{11}^{\mathrm{p}} - \dot{\varepsilon}_{22}^{\mathrm{p}}\right)^2 + \left(\dot{\varepsilon}_{22}^{\mathrm{p}} - \dot{\varepsilon}_{33}^{\mathrm{p}}\right)^2 + \left(\dot{\varepsilon}_{33}^{\mathrm{p}} - \dot{\varepsilon}_{11}^{\mathrm{p}}\right)^2 + 6\left(\dot{\varepsilon}_{12}^{\mathrm{p}^2} + \dot{\varepsilon}_{23}^{\mathrm{p}^2} + \dot{\varepsilon}_{31}^{\mathrm{p}^2}\right)\right)^{1/2}, \tag{17}$$

$$\sigma_{\mathrm{eff}} = \frac{1}{\sqrt{2}}\left((S_{11} - S_{22})^2 + (S_{22} - S_{33})^2 + (S_{33} - S_{11})^2 + 6\left(S_{12}^2 + S_{23}^2 + S_{31}^2\right)\right)^{1/2} \tag{18}$$

are the effective plastic strain rate and the effective stress, respectively.

In view of (16), rewrite Eq. (15) as

$$\dot{S}_{ij} = 2\mu\left(\dot{\varepsilon}_{ij}^{\mathrm{T}} - \frac{1}{3}\frac{\dot{V}}{V}\delta_{ij} - \frac{3}{2}\frac{\dot{\varepsilon}_{\mathrm{eff}}^{\mathrm{p}}}{\sigma_{\mathrm{eff}}} S_{ij}\right). \tag{19}$$

Eq. (19) implies that all components of the deviatoric stress tensor S_{ij} relax in similar fashion according to the effective stress relaxation.

To simulate the 2D deformation at the meso level, one has to solve a set of equations in x, y coordinates numerically. It includes:

the equations of motion

$$\rho\frac{\partial u_x}{\partial t}=\frac{\partial\sigma_{xx}}{\partial x}+\frac{\partial\sigma_{yx}}{\partial y},\quad \rho\frac{\partial u_y}{\partial t}=\frac{\partial\sigma_{xy}}{\partial x}+\frac{\partial\sigma_{yy}}{\partial y}, \tag{20}$$

the equation of continuity

$$\frac{\dot V}{V}=\dot\varepsilon_{xx}+\dot\varepsilon_{yy}+\dot\varepsilon_{zz}, \tag{21}$$

the equations for strain rates

$$\dot\varepsilon^{\mathrm{T}}_{xx}=\frac{\partial u_x}{\partial x},\quad \dot\varepsilon^{\mathrm{T}}_{yy}=\frac{\partial u_y}{\partial y},\quad \dot\varepsilon^{\mathrm{T}}_{xy}=\frac{1}{2}\left(\frac{\partial u_y}{\partial x}+\frac{\partial u_x}{\partial y}\right), \tag{22}$$

the constitutive equations

$$\dot\sigma_{xx}=-\dot P+\dot S_{xx},\quad \dot\sigma_{yy}=-\dot P+\dot S_{yy},\quad \dot\sigma_{xy}=\dot S_{xy}. \tag{23}$$

The subject under study is a meso volume loaded by weak shock waves and tension. In this case, heat effects are neglected and the medium may be considered as barotropic, that is, $P=P(\rho)$ or $P=P(\theta)$, where $\theta=\varepsilon^{\mathrm{e}}_{ii}$, ρ is the mass density. Hence, the set of equations (20)–(23) may be closed without the equation of conservation of energy (as the problems of dynamic elasticity). It is necessary, however, to note, that for this approach we have no information related to heat flow and temperature distributions. Based on the experimental data, equations of state have been constructed in [6] for a great number of materials.

Using constitutive equations of relaxation type (19) and viscous relaxation model of plastic strain rate (13), write deviatoric stress as

$$\dot S_{xx}=2\mu\left(\dot\varepsilon^{\mathrm{T}}_{xx}-\frac{1}{3}\frac{\dot V}{V}-\frac{1}{2\eta}\left(1-\frac{\sigma'_0}{\sigma_{\mathrm{eff}}}\right)S_{xx}\right),$$

$$\dot S_{yy}=2\mu\left(\dot\varepsilon^{\mathrm{T}}_{yy}-\frac{1}{3}\frac{\dot V}{V}-\frac{1}{2\eta}\left(1-\frac{\sigma'_0}{\sigma_{\mathrm{eff}}}\right)S_{yy}\right),$$

$$\dot S_{xy}=2\mu\left(\dot\varepsilon^{\mathrm{T}}_{xy}-\frac{1}{2\eta}\left(1-\frac{\sigma'_0}{\sigma_{\mathrm{eff}}}\right)S_{xy}\right). \tag{24}$$

Here the viscosity factor $\eta=\eta(\sigma_{\mathrm{eff}},\varepsilon^{\mathrm{p}}_{\mathrm{eff}})$ is defined by (14) and $\sigma'_0=\sigma'_0(\varepsilon^{\mathrm{p}}_{\mathrm{eff}})=2\tau'_0((4/3)\gamma^{\mathrm{p}})$ has a meaning of the current yield stress.

6. Calculation results

6.1. Modeling of uniform deformation

The deformation is assumed to be uniform macroscopically. The set of equations (10)–(17) was numerically solved under total strain rate. Fig. 1 shows the stress–strain curve under cyclic quasistatic loading with $\dot\varepsilon^{\mathrm{T}}_1=10^{-4}\ \mathrm{s}^{-1}$. It reflects all main peculiarities of material behavior under plastic deformation.

Stress–strain curves under quasistatic and dynamic loading at $\dot\varepsilon^{\mathrm{T}}_1=10^{-4}\ \mathrm{s}^{-1}$ and $\dot\varepsilon^{\mathrm{T}}_1=10^{4}\ \mathrm{s}^{-1}$, respectively, are presented in Fig. 2 in comparison with the experiment. Parameters of the model are defined by means of independent experiments, where the material microstructure is studied. These are presented in Table 1 for steel, Fe and Al6061-T6 with the average grain size $d_0=50,75,110$ μm and the average cell diameter of the cellular structure $d_{\mathrm{c}}=0.5,1,2$ μm, respectively.

6.2. 1D and 2D simulation of shock wave loading

To test the dislocation kinetics, a 1D problem was solved. The dislocation kinetics parameters

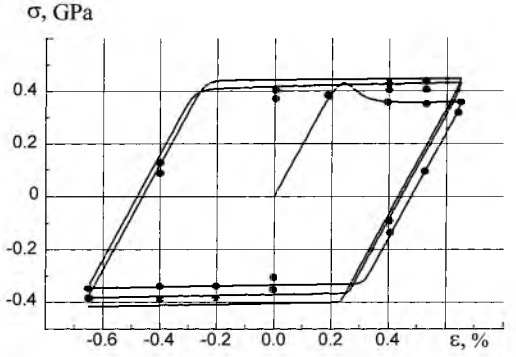

Fig. 1. Cyclic loading of the steel; • – experiment [7].

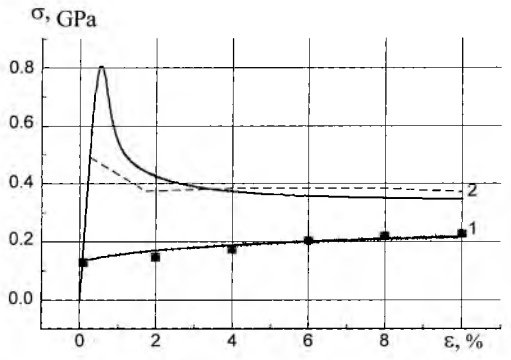

Fig. 2. Stress–strain curves for iron under different strain rates. (1) $\dot{\varepsilon} = 10^{-2}$ s^{-1}; (2) dynamic loading $\dot{\varepsilon} = 10^{4}$ s^{-1}. Dots and dashed lines – experiments [8].

were chosen to fit the experimental data for elastic precursor decay (Fig. 3). Then the results obtained were used to construct the function of relaxation time (or viscosity factor).

We consider a material meso volume, with the meso structure being taken into account in an explicit form. Grains, grain boundaries, inclusions of different type, pores, cracks, etc., may be considered as meso structure components. Such an approach allows us to study features of plastic deformation at the meso level: plastic strain localisation, movement of grains and grain blocks, formation and evolution of other meso fragments, which result in stress relaxation. As a first approximation, the meso volume of polycrystals is a conglomerate of grains distinguished by mechanical properties, such as yield points and relaxation time (Fig. 4).

2D calculations have shown that the qualitative strain pattern depends only slightly on the shock wave amplitudes. One observes only quantitative difference. We present here the results for meso volumes of aluminium alloy AL6061-T6 with different average grain size. The meso volume was shocked by 3.7 GPa.

A reference meso structure (Fig. 4(a)) determines the strain distribution in the meso volume and the formation and development of shear bands. However, notice that the strain degree in the shear bands increases as the shock wave moves away from the surface impacted. This is associated with the fact that the relaxation model describes the actual shape of the shock wave front, except the artificial viscosity mechanism. Immediately after collision a very steep and narrow shock wave front is formed near the surface impacted. This front is not capable of enveloping meso structure elements and of sensing the meso structure features; so, the bands of localised plastic strain near the surface impacted are rather a blur. However, high stress in the elastic precursor near the surface impacted result in intensive nucleation and motion of dislocations and fast stress relaxation. As the shock wave propagates away from the surface impacted, the front becomes progressively more gradual and wider due to development of plastic strain (Fig. 3). Then the shock wave front involves meso fragments (grains and grain groups) as a whole into motion. The plastic strain at the meso level manifests itself as the rotation of meso structure fragments (Fig. 4(b)) and shear band formation (Fig. 4(c)). In the case, when the width of a shock wave front and the average grain size are comparable, the shear bands are confined to the grain boundaries and the shear bands lie along all the grain boundaries (Fig. 4(c)).

6.3. 2D simulation of tension with different rates

The behavior of a meso volume of Al6061-T6 was investigated at different strain rates. Uniaxial

Table 1
Parameters of the dislocation model

Material	α	τ_0 (GPa)	N_0 (cm^{-2})	N^* (cm^{-2})	$\grave{A}$ (cm)	f_0	f^*	$\frac{B}{\lvert g\rvert b}$	β (GPa)
Steel	0.24	0.16	10^8	2×10^{11}	3.2	1	0.05	280	5
Fe	0.1	0.085	10^8	2×10^{10}	10	1	0.75	190	4
Al6061-T6	0.2	0.15	10^8	10^{11}	1.2	1	0.13	40	0.7

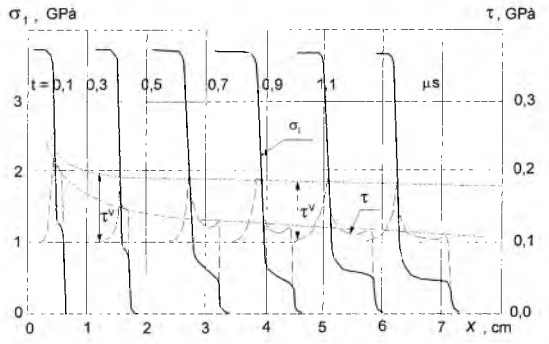

Fig. 3. The calculation of plane shock wave propagation in Al 6061-T6 with amplitude 3.7 GPa.

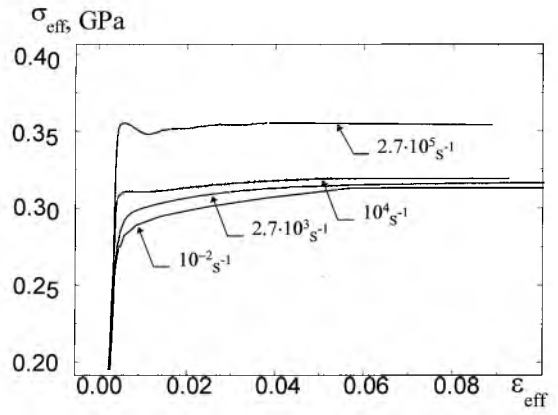

Fig. 5. Stress–strain curves of Al 6061-T6 under tension of different strain rates.

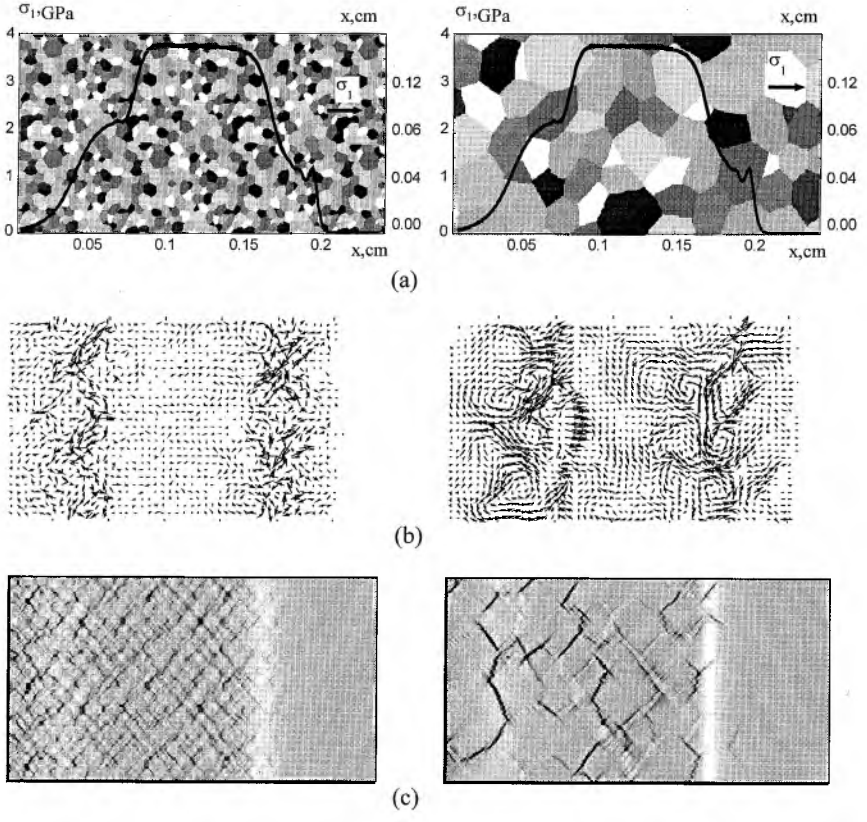

Fig. 4. Aluminium meso volumes shocked by 3.7 GPa: (a) calculated maps with different grain size (about 80 and 500 μm); (b) fields of particle velocities; (c) plastic strain distributions (■ – 4.5%, □ – 0–2%).

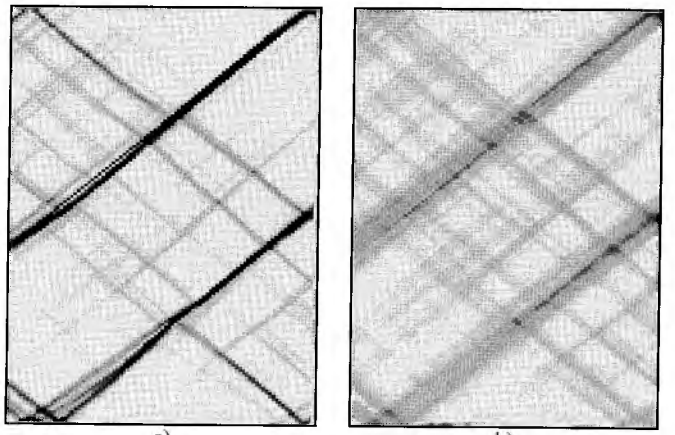

Fig. 6. Plastic strain distribution after stretching up to 3% (■ – 20%, ▨ – 0–0.7%) with (a) $\dot{\varepsilon} = 10^{-2}$ s^{-1} and (b) $\dot{\varepsilon} = 10^{4}$ s^{-1}.

tension was simulated by displacement of boundaries at a constant velocity. Fig. 5 shows the stress–strain curves, which are the total stress over all nodal points divided by the number of nodal points vs. percent elongation. The deformation rates were varied from $\dot{\varepsilon} = 10^{-2}$ s^{-1} to $\dot{\varepsilon} = 10^{5}$ s^{-1}. The calculations have shown that plastic strain distribution strongly depends on the strain rate. Low strain rates result in localisation of plastic deformation with clearly expressed shear bands which are shown in Fig. 6(a). The higher the strain rates the wider the bands of localised deformation (Fig. 6(b)). This was experimentally observed, e.g., in [2], and explained by the fact that a certain time is necessary for shear bands to be formed.

7. Conclusion

Constitutive relaxation equations have been constructed to simulate 1D and 2D deformation. The equations include both the stress relaxation and the strain hardening. All components of the deviatoric stress tensor relax in similar manner according to the effective stress relaxation. A reference meso structure was taken into consideration in an explicit form. 2D calculations have shown that the plastic strain at the meso level manifests itself as the rotation of meso structure fragments and shear band formation. The higher the strain rates the wider the bands of localised deformation.

References

[1] T.V. Zhukova, P.V. Makarov, T.M. Platova, The study of viscous and relaxation properties of metals in shock waves by mathematical modelling methods, Physics of Combustion and Explosion 23 (1) (1987) 29–35.

[2] L. Murr, D. Kuhlmann-Wilsdorf, Experimental and theoretical observations on the relationship between dislocation cell size, dislocation density, residual hardness, peak pressure and pulse duration in shock-loaded nickel, Acta Met. 26 (N5) (1978) 847–857.

[3] J. Gilman, Microdynamical theory of plasticity, in: Microplasticity, Metallurgiya, Moscow, 1972, pp. 18–37.

[4] P.V. Makarov, Elastoplastic deformation of metals by stress waves and the evolution of defective structure, Journal of Physics of Combustion and Explosion 23 (1) (1987) 22–29.

[5] M.L. Wilkins, Calculations of elastic–plastic flow, in: B. Alder, S. Fernbach, M. Rotenberg (Eds.), Methods in Computational Physics, vol. 3, Academic Press, New York, 1964, pp. 211–263.

[6] D. Wallace, Equation of state from weak shocks in solids, Physical review B 22 (N4) (1980) 1495–1502.

[7] L. Zbigniew, F. Kowalewski, M. Sliwowski, Effect of cyclic loading on the yield surface evolution of 18G2A low-alloy steel, International Journal of Mech. Science 39 (N1) (1997) 51–68.

[8] P. Pezhina, The Basic Questions of Viscous Plasticity, Mir, Moscow, 1968.